Journal of Earth Science, *Vol. 34*, *No. 1*, *p. 173−180*, *February 2023* ISSN 1674-487X
Printed in China
https://doi.org/10.1007/s12583-020-1115-2

Orbital and Millennial-Scale Climate Variability over the Past 76 ka in the Western Tarim Basin, Northwest China

Rui Zhang[1, 2, 3], Qiuzhen Yin[3], Weihua Nai[4], Zhixiang Wang[2], Hao Lu[3], Chunju Huang[*2, 5], Yansheng Gu[*2, 6], Lin Li[2], Yusong Wang[7], Linjing Liu[8]

1. *College of Urban and Environmental Sciences*, *Hubei Normal University*, *Huangshi* 435002, *China*
2. *State Key Laboratory of Biogeology and Environmental Geology*, *School of Earth Sciences*, *China University of Geosciences*, *Wuhan* 430074, *China*
3. *Georges Lemaître Centre for Earth and Climate Research*, *Earth and Life Institute*, *Université Catholique de Louvain*, *Louvain-La-Neuve* 1348, *Belgium*
4. *No.* 2 *Hydrological and Engineering Geology Party of Xinjiang Bureau of Geology and Mineral Resources Exploration and Development*, *Changji* 831100, *China*
5. *Hubei Key Laboratory of Critical Zone Evolution*, *School of Earth Sciences*, *China University of Geosciences*, *Wuhan* 430074, *China*
6. *Hubei Key Laboratory of Wetland Evolution & Eco-Restoration* (*WEER*), *China University of Geosciences*, *Wuhan* 430074, *China*
7. *School of Environmental Studies*, *China University of Geosciences*, *Wuhan* 430074, *China*
8. *Institute of Hydrogeology and Environmental Geology*, *Chinese Academy of Geological Sciences* (*CAGS*), *Shijiazhuang* 050061, *China*

Rui Zhang: https://orcid.org/0000-0001-9342-0271; Chunju Huang: http://orcid.org/0000-0002-9014-1282; Yansheng Gu: https://orcid.org/0000-0001-6620-1946

ABSTRACT: Paleoclimate changes during the last glacial in the arid central Asia are not as well understood as the monsoon-dominated areas of Asia. Here we report a 75-m-long sediment core over past 120 kyr based on astronomical tuning combined with the optically stimulated luminescence (OSL) dating in the Kashi depression of the western Tarim Basin, Northwest China. Analysis of grain size and high-resolution gamma ray (GR) logs from the KT11 borehole across the last glacial period yields a climate history for the Tarim Basin which reflects the variations of its temperature and the hydrological cycles. Comparison of these records with north hemisphere summer insolation, the Greenland ice core temperature, stalagmites and the loess from the nearby region indicates that the deposits in the fluvio-lacustrine system of the Kashi depression responded to climate change at the Younger Dryas (YD), six Heinrich cooling events and the Dansgaard-Oeschger cycles. Our work indicates that the alternations between warm-humid and cold-dry climates were prevalent in the western Tarim Basin during the last glacial period, showing an in-phase pattern with the climate variations of the East Asian Monsoon, controlled ultimately by precession and North Atlantic Ocean climate variability on orbital-millennial time scales.

KEY WORDS: abrupt climate changes, glacial geology, last glacial period, KT11 borehole, western Tarim Basin.

0 INTRODUCTION

The Tarim Basin is a part of the largest arid inland basin in central Asia. It is located in the southern part of the Xinjiang Uygur Autonomous Region, bounded by the Pamir Plateau to the west, the Lop Nur depression to the east, Tian Shan Mountains to the north, and the Kunlun Mountains to the south (Sun et al., 2017). The Tarim Basin has limited water resources, scarce vegetation and fragile ecosystems, making it a crucial site for studying the climate change in the Asian interior (Chen et al., 2016). Westerlies has an impact on the climate changes of the western China, especially in the inland arid Tarim Basin (Chang et al., 2017). Previous research has focused on Holocene climate variability in the Tarim Basin and the related driving mechanisms (Zhao et al., 2012), but paleoclimate changes during the last glacial in the western Tarim Basin and surrounding areas are poorly understood and their relationship with climate changes related to the monsoonal in China and other regions is still unclear.

The Last Glacial Period was characterized by abrupt millennial-scale climate variability that is well revealed by high-resolution ice cores and marine sediments (Dansgaard et al., 1993; Heinrich, 1988). These high-frequency climate oscil-

*Corresponding author: huangcj@cug.edu.cn; ysgu@cug.edu.cn

Manuscript received July 12, 2020.
Manuscript accepted October 13, 2020.

Zhang Rui, Yin Qiuzhen, Nai Weihua, Wang Zhixiang, Lu Hao, Huang Chunju, Gu Yansheng, Li Lin, Wang Yusong, Liu Linjing, 2023. Orbital and Millennial-Scale Climate Variability over the Past 76 ka in the Western Tarim Basin, Northwest China. *Journal of Earth Science*, 34(1): 173–180. https://doi.org/10.1007/s12583-020-1115-2. http://en.earth-science.net

lations of rapid warming followed by slower cooling are identified as ca. 1.5-kyr duration shifts in the $\delta^{18}O$ record from the Greenland ice cores, and are now known as Dansgaard-Oeschger (D-O) cycles (NGRIP Members, 2004; Bond et al., 1999). Some of the cold stadials were also characterized by Heinrich events (H), indicative of massive discharge of icebergs into the North Atlantic (Hemming, 2004; Bond et al., 1993; Heinrich, 1988). Millennial-scale climate H events and D-O cycles within Last Glacial have been identified worldwide in various geological archives throughout the northern Hemisphere (Liu et al., 2020; Wang et al., 2018; Lin et al., 2010; Shakun and Carlson, 2010; Jiménez-Moreno et al., 2008, 2007; Alley et al., 1997). Models for the forcing mechanisms of these millennial-scale events include linkages with Atlantic meridional overturning circulation (AMOC; Sun et al., 2012; Bond et al., 1993). Similar millennial-scale climate events have been found in numerous terrestrial archives from the northern Hemisphere, including lake sediments, speleothems and loess (Wang et al., 2018, 2002). The northern westerlies played an important role in transmitting the signal from the North Atlantic to the central Asia during the Last Glacial (Li Y et al., 2016).

Although the fluvial sedimentary records are prone to short-term deposition pulses and erosion at different scales, some sequences in fluvial facies have been shown to record sedimentological expression of Heinrich events (López-García et al., 2013; Macklin et al., 2002). Millennial-scale paleoclimate changes are expected in records from arid central Asia. Indeed, several studies (Li et al., 2019; Wang et al., 2018) have documented H events and D-O cycles in the westerlies-dominated area during the last glacial and interglacial. In that region, the central Asian loess results from transportation by the westerlies responding to climatic teleconnection links to the North Atlantic (Wang et al., 2018). However, there is not much research about the sequences within inland fluvio-lacustrine systems in arid central Asia. Thus, an interesting question is whether and how these inland fluvio-lacustrine systems responded to global climate changes during the last glacial period, especially to millennial-scale H events and D-O cycles.

In this study, we obtained the age constraints from optically stimulated luminescence (OSL) dating and astronomical tuning of the 75-m KT11 borehole in order to reconstruct orbital and millennial-scale climate fluctuations over the past 76 ka in the westernmost Tarim Basin. These data will help to better understand the forcing mechanisms of climate change in arid regions and their implications.

1 MATERIALS AND METHODS

1.1 Geological Setting and Drilling

The Kashi depression located at the most western of Tarim Basin (Fig. 1). The regional climate here is mainly controlled by westerly (Aizen et al., 2006) and dominated by a temperate desert climate. Vegetation here is dominated by semi-desert and steppe types (XET-CAS, 1978). More information about Kashi depression could be found in Zhang et al. (2019).

Core KT11 (39°17′39″N, 76°32′19″E, 1 230 m above sea level) was drilled by the XY-6N drill tower in Kashi depression in the July, 2017 (Zhang et al., 2019). For the 15.5 m above, there exits disturbance when drilling, and there is also no OSL dating. Thus, we did not discuss this part. The 75-m (90–15.5 m) succession can be divided into 3 lithologic units based on variations in color and grain-size. Lower Unit 1 (90–61 m) mainly consists of grayish silt clay with a grayish silt layer, a grayish clay layer and a grayish yellow silty clay. Middle Unit 2 (61–39.8 m) is marked by grayish silt with a grayish-yellow fine sand layer and a grayish silty clay. Upper Unit 3 (39.8–15.5 m) is grayish silty clay interbedded with grayish-yellow fine sand and a grayish clay. From this core, there is lack of coarse-grained gravels and showing the very uniform fine sand, therefore, we interpret that the grayish-yellow sand layers were deposited in an arid fluvial-delta environment. And the grayish silt/clay were deposited in a high marginal lake environment.

1.2 Optically Stimulated Luminescence (OSL) Dating

For this study, 8 cylindrical samples (10 cm long, 12 cm diameter) of mainly medium- to fine-grained sand were collected from 44.48–18.50 m interval and kept in black plastic bags in preparation for optically stimulated luminescence (OSL) dating. OSL measurements were performed using a Daybreak 2200 TL/OSL automatic system in the OSL laboratory of the Institute of Hydrogeology and Environmental Geology, Chinese Academy of Geological Sciences in Shijiazhuang City. All samples' preparations were conducted under subdued red light and followed the procedures outlined by Liu et al. (2015). The outer 3–4 cm of sediment in each sample was removed and the middle portion was used for further processing, which involved pretreatment with 30% HCl to remove carbonate and 40% H_2O_2 to remove organic matter. They were then treated with 30% hydrofluorosilicic acid (H_2SiF_6) for 5 days to dissolve feldspars. After that, fine quartz grains in the size range 4–11 μm were selected and deposited on stainless steel discs.

Irradiations were carried out using a $^{90}Sr/^{90}Y$ beta source delivering 0.08 Gy/Sec. The concentrations of U, Th and K were measured by neutron activation analysis, and the water contents were measured by weighing the samples before and after drying (Liu et al., 2015).

1.3 Measurement of Gamma-Ray and Grain-Size

For grain-size measurements, 47 samples were collected from the KT11 core between 60 and 17 m with an interval of approximate 0.75 m. For each sample, about 0.5 g of powder was pretreated using 10% H_2O_2 to remove organic matter, and treated with 10% HCl to remove carbonates, then rinsed repeatedly with ultrapure water to remove acid residue. The residues were dispersed with 10% $(NaPO_3)_6$ and ultrasonicated for 3–5 min. The grain-size measurements were carried out by a Malvern Mastersizer 3000 laser grain-size analyzer (Gu et al., 2018). All of above measurements were made in Hubei Key Laboratory of Wetland Evolution & Eco-Restoration (WEER), China University of Geosciences (Wuhan).

Gamma-ray (GR) logging of the KT11 borehole was obtained by a JHQ-2D Comprehensive CNC logging system in the field at 0.05-m intervals downhole (Zhang et al., 2019). It is widely used for both interpreting paleoenvironmental conditions and analyzing climate forcing (Li M S et al., 2016; Wu et

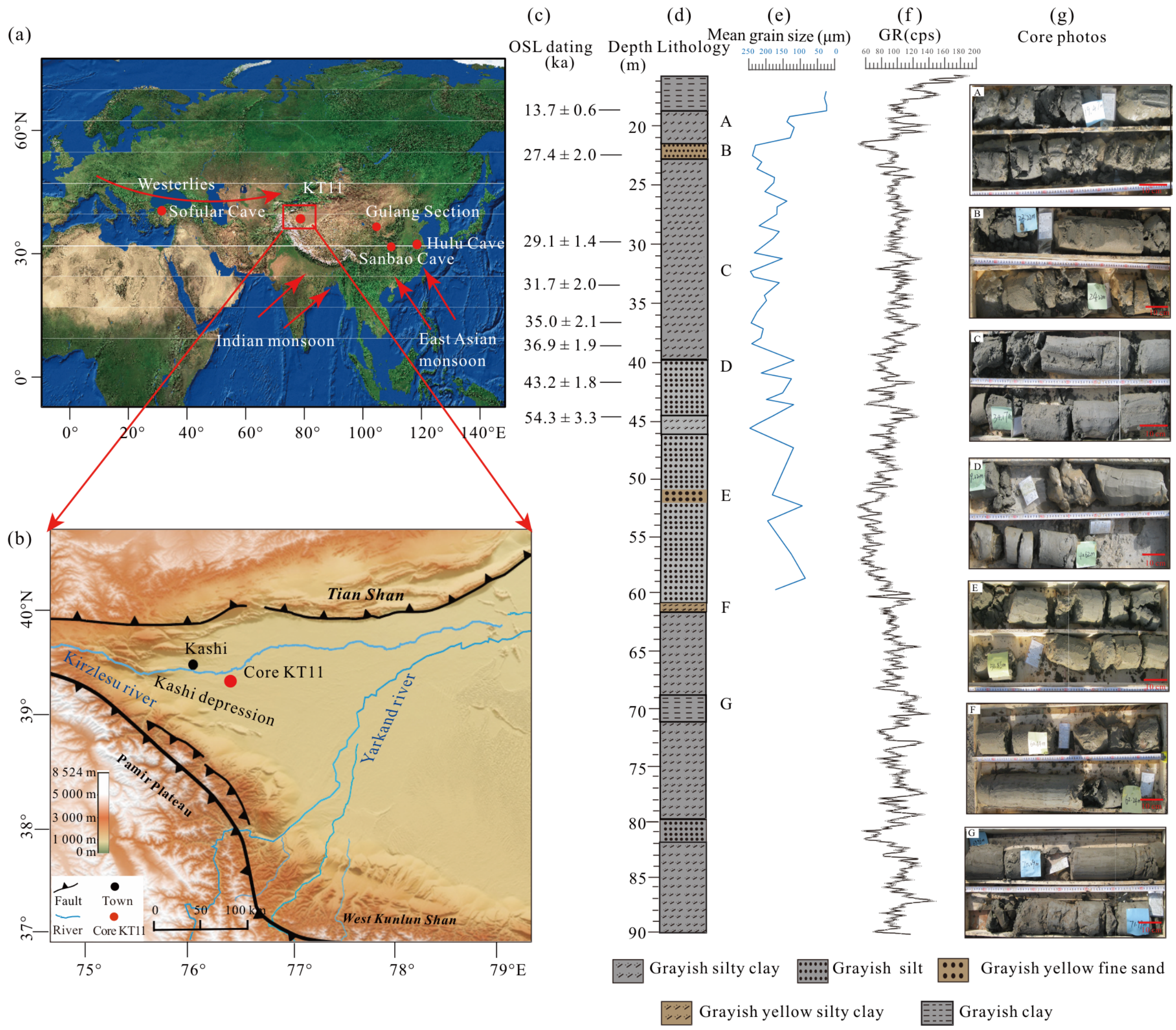

Figure 1. (a) Satellite map from Google Earth with red dots showing locations of borehole KT11, of Sanbao, Hulu and Sofular caves and of the Gulang Section. (b) Kashi depression with borehole KT11 marked with a red dot, modified from Zheng et al. (2015). (c) OSL dating results, (d) lithology, (e) mean grain size, (f) logs of GR and (g) visual borehole imagery of borehole KT11.

al., 2013; Carter and Gammon, 2004). The GR log represents the radioactive intensity of sediments, dominated by the amount of K, U and Th in the rock, and these elements associated with clay and organic-rich lithologies (Schnyder et al., 2006). For the continental deposit, variations in gamma-ray (GR) are mainly affected by relative clay to sand ratios in the sediment, which in turn are often linked with the intensity of terrestrial weathering and runoff in the watershed regions (Li et al., 2017; Wu et al., 2013). Therefore, in the 90–15.5 m interval of borehole KT11, high GR values are generally linked with clay-rich sediments and lower GR values are usually attributed to coarser-grained sand (Zhang et al., 2019). The GR data show a negative correlation with mean grain-size series (Figs. 1e and 1f).

1.4 Time-Series Method

Cyclostratigraphic analysis was carry out on the KT11 GR series using the Acycle software (Li M S et al., 2018). The GR series was resampled, then prewhitened by subtracting a 35% weighted averaged to remove long-term trends and highlight high frequency astronomical parameters in the precession band in the power spectrum. Finally, spectral analysis on both the untuned GR series in depth and tuned data followed the same procedures used in Zhang et al. (2019).

2 CHRONOLOGY OF CORE KT11

2.1 OSL Dating

The OSL ages obtained from quartz are in stratigraphic order from 54.3 ± 3.3 to 13.7 ± 0.6 ka (Table 1). The average sedimentation rate was 65 cm/kyr between 44.48–18.50 m based on the OSL dating, but with changes in average accumulation rate at 23.3, 29.75 and 38.45 m. Here we choose the OSL dating results at 23.3 and 29.75 m as the anchors.

2.2 Spectral Analysis and Timescale Development

The power spectrum of the GR series which are subtracted a 35% weighted average shows a clear and significant (>99% confidence level) peak at ~16 m, and a weaker but still >99% confidence peak at ~7.7 m (Fig. 2e). Based on OSL dating, coupled with a previously published age for the KT11

Table 1 Comparison OSL dating results of samples with the astronomical time scale (ATS)

Depth (m)	U (ppm)	Th (ppm)	K (%)	De (Gy)	Dose rate (Gy/kyr)	Water content (%)	Age (ka)	ATS (ka)
18.50	3.42	15.70	2.44	64.35 ± 1.42	4.71 ± 0.19	21.5	13.7 ± 0.6	14.8
23.30	2.16	10.21	1.75	98.20 ± 5.48	3.21 ± 0.13	19.7	27.4 ± 2.0	25.4
29.75	2.38	16.24	1.83	118.36 ± 3.25	4.07 ± 0.16	11.6	29.1 ± 1.4	29.1
33.55	2.52	17.20	1.85	133.86 ± 7.61	4.22 ± 0.17	12.0	31.7 ± 2.0	33.9
36.70	3.01	16.66	1.79	142.98 ± 6.41	4.08 ± 0.16	19.8	35.0 ± 2.1	37.8
38.45	2.28	15.81	1.50	133.43 ± 4.58	3.61 ± 0.14	14.9	36.9 ± 1.9	40
41.80	2.83	11.59	1.59	148.99 ± 1.24	3.45 ± 0.14	16.0	43.2 ± 1.8	45.3
44.48	2.20	20.19	1.66	223.93 ± 10.16	4.12 ± 0.16	14.8	54.3 ± 3.3	50

core in Zhang et al. (2019), the average accumulation rate for 90–15 m interval is about 65–70 cm·kyr^{-1}. Thus, according to this sedimentation rate, the ~16 m wavelength cycle we recognized from our spectral analysis should corresponds to ~23 kyr precession cycles, and the ~7.7 m wavelength should correspond to half-precession cycles. The ~16 m (~23 kyr) cycles dominate the variance of the record, and we thus tuned the GR series to these cycles to generate an age model. In total, ~5 cycles can be recognized at this wavelength, yielding a ~118 kyr astronomical timescale. The power spectrum of the 23 kyr-tuned data shows significant peaks at 23 and 11.5 kyr periods (Fig. 2f). Considering the OSL dating at 29.75 and 23.3 m as the anchors, the 23 kyr tuned GR time series provides a 118 kyr astronomical timescale from 9 to 127 ka, and this age model is consistent with the other six OSL dating results (Table 1).

3 DISCUSSION

3.1 Orbital-Scale Climatic Variability in the Western Tarim Basin

Based on our astronomical tuning coupled with the OSL dating anchor points, we obtained a tuned astronomical timescale for the KT11 core spanning 127 to 9 ka across the 90–15.5 m interval. Combined the mean grain size data, we try to discuss the climatic variabilities during last glacial period. At the orbital timescale, the variations of the GR series from the core KT11 of the Kashi depression shows a good correlation with local (northern Hemisphere 39°) summer insolation (Berger, 1978) (Fig. 3), with a strong precession cycle. The Kashi depression is in arid central Asia where westerlies are dominant, and previous studies have also shown that there is a strong control of precession on loess records in this region (Li Y et al., 2019, 2016; Wang et al., 2018). Model results also show that precession and insolation control variations in the westerlies on orbital time scales (Li et al., 2019), which in turn enables transmission of the processional signals to the West Tarim Basin. These models show northward shift of the westerlies corresponding to smaller precession index (higher summer insolation) (Li et al., 2019). In our study, precession and insolation modulate the long-term change of the GR proxy, with higher summer insolation corresponding to higher GR values.

Rao et al. (2019) emphasized the relationships between temperature and internal processes on the hydrological cycles in the Xinjiang region during the Holocene. Similarly, we suggest that temperature and hydrology played important roles in the climate variability in the Kashi depression during the 76–9 ka internal. During warmer intervals related to higher insolation, the snow and ice melted, water runoff intensified, evapotranspiration and the moisture cycle were enhanced together with together with the consequent rise of lake levels. More humid condition coupled with higher temperature would result in more chemical weathering, and eventually, more clay being washed downstream into the fluvio-lacustrine system of the Kashi depression. In contrast, a colder condition in Kashi would result in more semi-arid climate and produce less clay but relatively sand-rich, hence lower GR values but increased mean grain size. Thus, we interpret our GR record from the KT11 borehole in westernmost Tarim Basin as reflecting a warm-humid climate during interstadials and a cold-dry climate during stadials.

The precise relationship of the climate vairaitons between the arid central Asia (ACA) and the monsoonal Asia region at different time scales is always a controvesial. For example, based on comparison between lake sediments and loess deposits, Chen et al. (2019, 2016) proposed that precipitation/ moisture variations during the Holocene in arid central Asia are out of phase/anti-phased with those in mid-latitude monsoonal Asia. The magnetic properties and grain size record from loess during Marine Isotope Stage 5 (MIS 5) from the Yili Valley, which was interpreted to imply precipitation changes in central Asia, was found to be out-of-phase with the intensity of the Asian Monsoon because of corresponding movements in pressure and rain belts (Jia et al., 2018). The arid central Asia climate was also characterized by a cold-moist and warm-dry pattern during sub-stages of MIS 5 based on loess-paleosol sequence from the Tian Shan Mountains, reflecting an anti-phase relationship to that in monsoonal East Asia which may be caused by the insolation gradient (Li G Q et al., 2018). However, the magnetic susceptibility records from Tajikistan Loess deposits during the Last Glacial suggest that there were humid interstadial and dry stadial climate oscillations in this part of central Asia, which were in-phase with the intensity of the mid-latitude Asian Monsoon (Wang et al., 2018). Similar to this study, our GR record shows an in-phase relationship with speleothem records from monsoonal China on orbital time scales during last glacial period (Fig. 3).

3.2 Millennial-Scale Climatic Variability in the Western Tarim Basin

On millennial timescale, the variability in the GR series and mean grain size records match well with the NGRIP ice

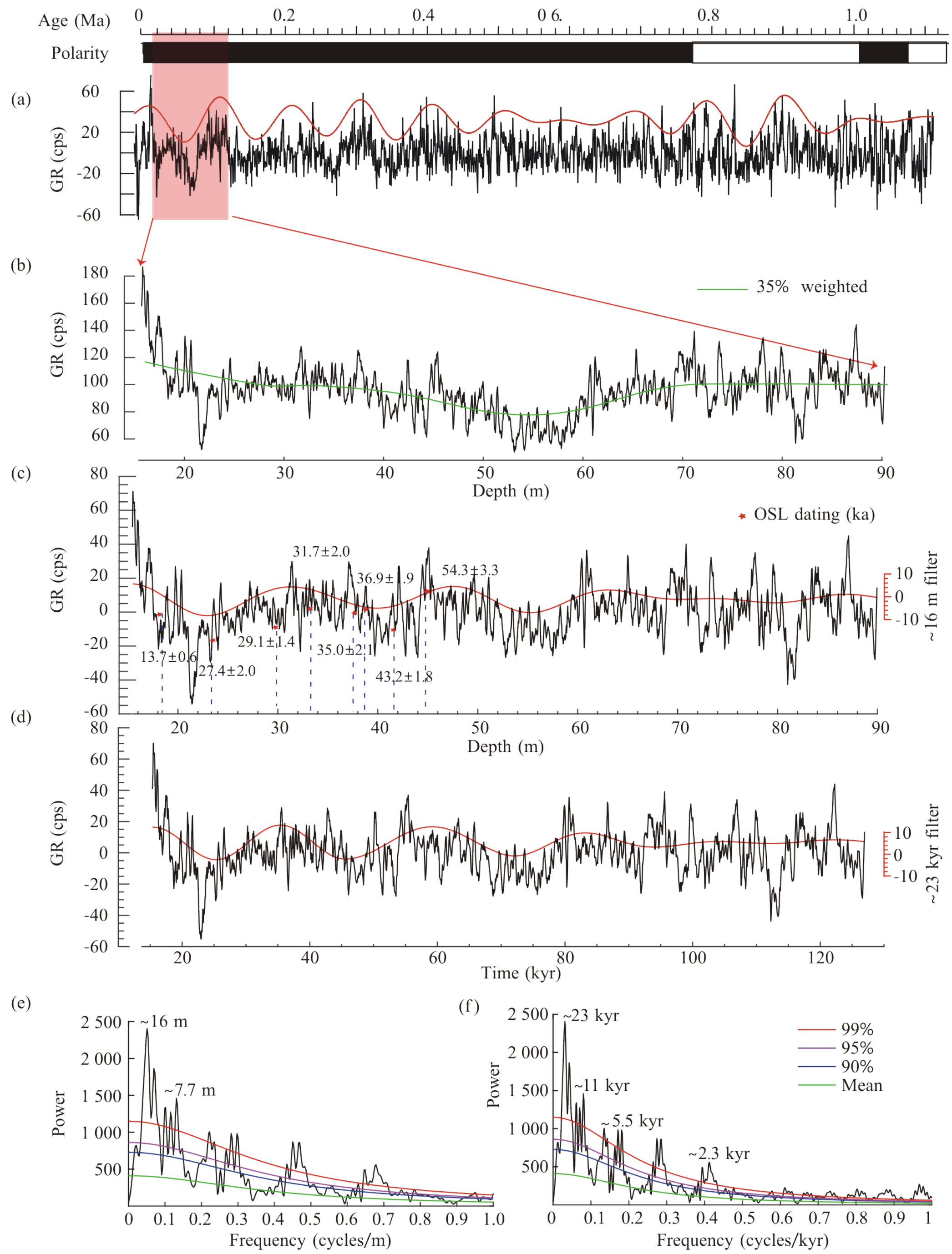

Figure 2. Interpreted cyclostratigraphy and spectral analysis results of the core KT11. (a) GR series from the total 800 m core KT11; (b) the GR series (black line) with 35% average weighted curve shown (green line); (c) GR data with ~16 m filtered cycles (red line) after subtracting the 35% weighted average (Gauss filter; band-pass of 0.06 ± 0.02 cycles/cm); (d) the ~23 kyr tuned GR series after subtraction of 35% weighted average, with filtered ~23 kyr cycles (red line) (Gauss filter, band-pass: 0.044 ± 0.008 cycles/kyr); (e) 2π MTM power spectra of GR series in depth; (f) 2π MTM power spectra of the ~23 kyr tuned GR series.

core (NGRIP Members, 2004), the Sanbao/Hulu stalagmites $\delta^{18}O$ records from central China (Wang et al., 2008), the Sofular Cave $\delta^{13}C$ records from northern Turkey (Fleitmann et al., 2009) and the Chinese Loess Plateau grain size record (Sun et al., 2012) (Fig. 3; see Fig. 1a for locations). Within the dating uncertainties, our records from the KT11 core indicate that Heinrich events H6-H1 and the Younger Dryas (Fig. 3) are expressed, which can be considered as the most characteristic example of millennial-scale climate variability during Last Glacial (Naafs et al., 2013). These results suggest that the millennial-scale climate changes in the westernmost Tarim Basin are indicative of a teleconnection to the North Atlantic Ocean climate oscillations during last glacial, or indeed that both regions are responding to a common driving factor, such as solar forcing. Regardless of the precise mechanistic relationship, there appears to be a climatic coupling between central and East Asia and the North Atlantic. Wu et al. (2008) demonstrated that the shutdown of the Atlantic Meridional Overturning Circula-

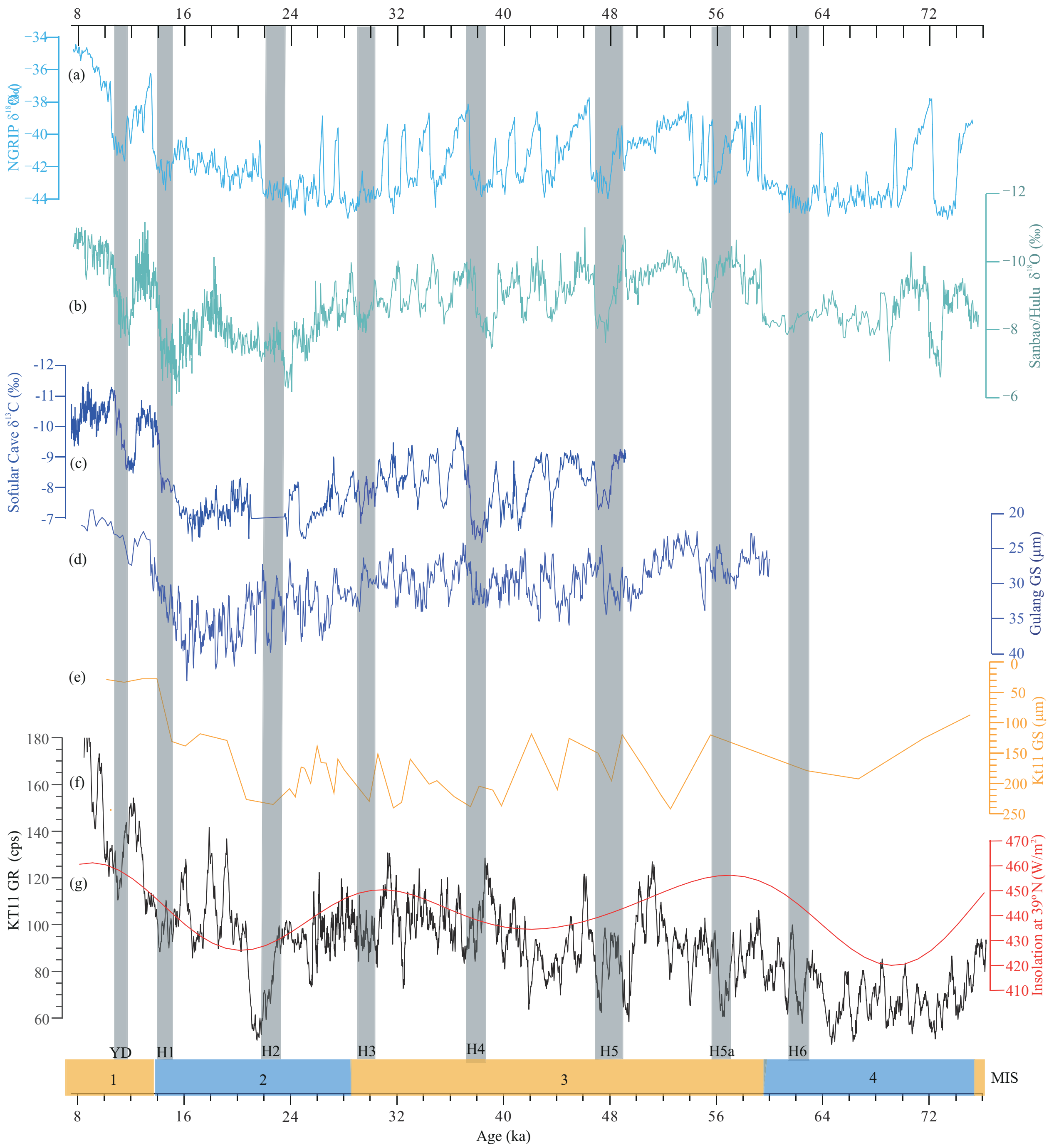

Figure 3. Millennial-scale climate change for the 76–9 ka interval on Kashi depression. Comparison of the GR data and mean grain size from the KT11 borehole with other climate records. (a) The variations in $\delta^{18}O$ composition in the NGRIP ice record, Greenland (NGRIP Members, 2004); (b) Sanbao/Hulu speleothem $\delta^{18}O$ records (Wang et al., 2008); (c) Sofular Cave $\delta^{13}C$ records (Fleitmann et al., 2009); (d) the Chinese Loess Plateau grain size record (Gulang Section, Sun et al., 2012); (e) the mean grain size record of the KT11; (f) summer insolation at 39°N (Berger, 1978); (g) GR data from the KT11 core (this study). H1 to H6 represent positions of Heinrich events (Bond et al., 1993), the yellow and blue color bars represent the odd and even Marine Isotope Stages, respectively.

tion (AMOC) leads to an intense cooling in the extratropical North Atlantic and also a widespread response over the global ocean. These processes may have exported the effect to the westernmost Tarim Basin. Then during these cold internals, evapotranspiration could be weakened and the moisture cycle and water runoff reduced in the Kashi region. These would result in less chemical weathering and a decreased clay influx into the Kashi depression as recorded by low-GR but increased-mean grain size (Fig. 3).

The GR record of the KT11 borehole has several additional peaks between the interpreted H events conditions. These may seem to be correlated to the D-O events, which are rapid alternations between cold and warm conditions in Greenland (winter) air temperature recorded in ice cores. Nevertheless, without further very high-resolution dating, we cannot precisely match the peaks from our GR data with the NGRIP ice record.

4 CONCLUSIONS

OSL dating and astronomical tuning have been used to establish a robust high resolution chronology for the KT11 borehole fluvio-lacustrine sediments from the Kashi depression during the last glacial period. The GR log (reflecting relative clay to sand abundances) records increased clay sedimentation during warm-humid conditions alternating with coarser sedimentation during cool-arid climates. The GR and mean grain size data reveal that the influence of temperature and the hydrological cycles play significant role on the climate in Xinjiang region, and supports the view that climate variations have an in-phase relationship between central Asia and mid-latitude monsoonal Asia during last glacial period.

The GR record has a good correlation with summer insolation. Six of the Heinrich, Younger Dryas cold events and D-O cycles of the last glacial also appear to be recorded by the fluvio-lacustrine system on the Kashi depression. This demonstrates that rapid and high frequency climate changes in the North Atlantic also had profound climate effects on the western Tarim Basin region.

ACKNOWLEDGMENTS

This work was supported by the National Natural Science Foundation of China (Nos. 41772029, 41322013), Natural Science Foundation for Distinguished Young Scholars of Hubei Province of China (No. 2016CFA051), the Program of Introducing Talents of Discipline to Universities (Nos. B14031, B08030), the Fundamental Research Funds for the Central Universities, China University of Geosciences (Wuhan) (Nos. CUGCJ1703, CUGQYZX1705) and Hydrogeological Environmental Geological Survey of Kashi, Xinjiang (No. S15-2-LQ1). Qiuzhen Yin thanks the support of Fonds de la Recherche Scientifique-FNRS. We thank Yuchuan Mi, Shuqi Yu, Shuo Guan and Yue Gao (Chinese University of Geosciences in Wuhan) for their assistance with field sampling. We also thank Chengmin Wang (Institute of Hydrogeology and Environmental Geology in Shijiazhuang) for help in experiment. We are grateful to Professor David Kemp (Chinese University of Geosciences in Wuhan) and James Ogg (Purdue University) for discussing the science interpretations and helping with the English style that notably improved the manuscript. The final publication is available at Springer via https://doi.org/10.1007/s12583-020-1115-2.

REFERENCES CITED

Alley, R. B., Mayewski, P. A., Sowers, T., et al., 1997. Holocene Climatic Instability: A Prominent, Widespread Event 8 200 yr ago. *Geology*, 25 (6): 483–486. https://doi .org/10.1130/0091-7613(1997)0250483:hciapw>2.3.co;2

Aizen, V. B., Aizen, E. M., Joswiak, D. R., et al., 2006. Climatic and Atmospheric Circulation Pattern Variability from Ice-Core Isotope/Geochemistry Records (Altai, Tien Shan and Tibet). *Annals of Glaciology*, 43: 49–60. https://doi.org/10.3189/172756406781812078

Berger, A., 1978. Long-Term Variations of Daily Insolation and Quaternary Climatic Changes. *Journal of the Atmospheric Sciences*, 35(12): 2362–2367. https://doi.org/10.1175/1520-0469(1978)0352362:ltvodi>2.0.co;2

Bond, G., Broecker, W., Johnsen, S., et al., 1993. Correlations between Climate Records from North Atlantic Sediments and Greenland Ice. *Nature*, 365(6442): 143–147. https://doi.org/10.1038/365143a0

Bond, G. C., Showers, W., Elliot, M., et al., 1999. The North Atlantic's 1–2 kyr Climate Rhythm: Relation to Heinrich Events, Dansgaard/Oeschger Cycles and the Little Ice Age. Mechanisms of Global Climate Change at Millennial Time Scales. American Geophysical Union, Washington, D.C.. 35–58. https://doi.org/10.1029/gm112p0035

Carter, R. M., Gammon, P., 2004. New Zealand Maritime Glaciation: Millennial-Scale Southern Climate Change since 3.9 Ma. *Science*, 304 (5677): 1659–1662. https://doi.org/10.1126/science.1093726

Chang, H., An, Z. S., Wu, F., et al., 2017. Late Miocene–Early Pleistocene Climate Change in the Mid-Latitude Westerlies and Their Influence on Asian Monsoon as Constrained by the K/Al Ratio Record from Drill Core Ls2 in the Tarim Basin. *Catena*, 153: 75 – 82. https://doi.org/10.1016/j.catena.2017.02.002

Chen, F. H., Chen, J. H., Huang, W., et al., 2019. Westerlies Asia and Monsoonal Asia: Spatiotemporal Differences in Climate Change and Possible Mechanisms on Decadal to Sub-Orbital Timescales. *Earth-Science Reviews*, 192: 337–354. https://doi.org/10.1016/j.earscirev.2019.03.005

Chen, F. H., Jia, J., Chen, J. H., et al., 2016. A Persistent Holocene Wetting Trend in Arid Central Asia, with Wettest Conditions in the Late Holocene, Revealed by Multi-Proxy Analyses of Loess-Paleosol Sequences in Xinjiang, China. *Quaternary Science Reviews*, 146: 134–146. https://doi.org/10.1016/j.quascirev.2016.06.002

Dansgaard, W., Johnsen, S. J., Clausen, H. B., et al., 1993. Evidence for General Instability of Past Climate from a 250-kyr Ice-Core Record. *Nature*, 364(6434): 218–220. https://doi.org/10.1038/364218a0

Fleitmann, D., Cheng, H., Badertscher, S., et al., 2009. Timing and Climatic Impact of Greenland Interstadials Recorded in Stalagmites from Northern Turkey. *Geophysical Research Letters*, 36(19): L19707. https://doi.org/10.1029/2009gl040050

Gu, Y. S., Guan, S., Ma, T., et al., 2018. Quaternary Sedimentary Environment Documented by Borehole Stratigraphical Records in Eastern Jianghan Basin. *Earth Science*, 43(11): 3989–4000. https://doi.org/10.3799/dqkx.2018.324 (in Chinese with English Abstract)

Heinrich, H., 1988. Origin and Consequences of Cyclic Ice Rafting in the Northeast Atlantic Ocean during the Past 130 000 Years. *Quaternary Research*, 29(2): 142 – 152. https://doi.org/10.1016/0033-5894(88)90057-9

Hemming, S. R., 2004. Heinrich Events: Massive Late Pleistocene Detritus Layers of the North Atlantic and Their Global Climate Imprint. *Reviews of Geophysics*, 42(1): 1005. https://doi .org/10.1029/2003rg000128

Jia, J, Gao, F. Y., Xia, D. S., et al. 2018. Moisture Variations in Arid Central Asia and Its Out-of-Phase Relationship with the Asian Monsoon during MIS 5: Evidence from Loess Records. *Journal of Quaternary Science*, 33: 435–443. https://10.1016/j.quascirev.2007.10.017

Jiménez-Moreno, G., Fawcett, P. J., Scott Anderson, R., 2008. Millennial- and Centennial-Scale Vegetation and Climate Changes during the Late Pleistocene and Holocene from Northern New Mexico (USA). *Quaternary Science Reviews*, 27(13/14): 1442 – 1452. https://doi. org/10.1016/j.quascirev.2008.04.004

Jiménez-Moreno, G., Scott Anderson, R., Fawcett, P. J., 2007. Orbital- and Millennial-Scale Vegetation and Climate Changes of the Past 225 ka from Bear Lake, Utah-Idaho (USA). *Quaternary Science Reviews*, 26 (13/14): 1713–1724. https://doi.org/10.1016/j.quascirev.2007.05.001

Li, G. Q., Chen, F. H., Xia, D. S., et al., 2018. A Tianshan Mountains Loess-

Paleosol Sequence Indicates Anti-Phase Climatic Variations in Arid Central Asia and in East Asia. *Earth and Planetary Science Letters*, 494: 153–163. https://doi.org/10.1016/j.epsl.2018.04.052

Li, M. S., Kump, L., Hinnov, L. A., et al., 2018. Tracking Variable Sedimentation Rates and Astronomical Forcing in Phanerozoic Paleoclimate Proxy Series with Evolutionary Correlation Coefficients and Hypothesis Testing. *Earth and Planetary Science Letters*, 501: 165–179. https://doi.org/10.1016/j.epsl.2018.08.041

Li, M. S., Ogg, J., Zhang, Y., et al., 2016. Astronomical Tuning of the End-Permian Extinction and the Early Triassic Epoch of South China and Germany. *Earth and Planetary Science Letters*, 441: 10–25. https://doi.org/10.1016/j.epsl.2016.02.017

Li, M. S., Zhang, Y., Huang, C. J., et al., 2017. Astronomical Tuning and Magnetostratigraphy of the Upper Triassic Xujiahe Formation of South China and Newark Supergroup of North America: Implications for the Late Triassic Time Scale. *Earth and Planetary Science Letters*, 475: 207–223. https://doi.org/10.1016/j.epsl.2017.07.015

Li, Y., Song, Y. G., Lai, Z. P., et al., 2016. Rapid and Cyclic Dust Accumulation during MIS 2 in Central Asia Inferred from Loess OSL Dating and Grain-Size Analysis. *Scientific Reports*, 6: 32365. https://doi.org/10.1038/srep32365

Li, Y., Song, Y. G., Yin, Q. Z., et al., 2019. Orbital and Millennial Northern Mid-Latitude Westerlies over the last Glacial Period. *Climate Dynamics*, 53(5): 3315–3324. https://doi.org/10.1007/s00382-019-04704-5

Lin, X., Chang, H., Li, Y. T., et al., 2010. Rapid Paleoclimate Changes during MIS3a Reflected by Lacustrine Deposits of Dujiangyan in the Eastern Margin of Qinghai-Tibet Plateau. *Earth Science*, 35(5): 857–866. http://doi.org/10.3799/dqkx.2010.099 (in Chinese with English Abstract)

Liu, X. X., Sun, Y. B., Vandenberghe, J., et al., 2020. Centennial- to Millennial-Scale Monsoon Changes since the last Deglaciation Linked to Solar Activities and North Atlantic Cooling. *Climate of the Past*, 16 (1): 315–324. https://doi.org/10.5194/cp-16-315-2020

Liu, Z., Zhao, H., Wang, C. M., et al., 2015. Estimation of Paleo-Firing Temperatures Using Luminescence Signals for the Volcanic Lava Baked Layer in Datong, China. *Quaternary Geochronology*, 30: 363–368. https://doi.org/10.1016/j.quageo.2015.06.010

López-García, J. M., Blain, H. A., Bennàsar, M., et al., 2013. Heinrich Event 4 Characterized by Terrestrial Proxies in Southwestern Europe. *Climate of the Past*, 9(3): 1053–1064

Macklin, M. G., Fuller, I. C., Lewin, J., et al., 2002. Correlation of Fluvial Sequences in the Mediterranean Basin over the Last 200 ka and Their Relationship to Climate Change. *Quaternary Science Reviews*, 21(14/15): 1633–1641. https://doi.org/10.1016/S0277-3791(01)00147-0

Naafs, B. D. A., Hefter, J., Stein, R., 2013. Millennial-Scale Ice Rafting Events and Hudson Strait Heinrich(-Like) Events during the Late Pliocene and Pleistocene: A Review. *Quaternary Science Reviews*, 80: 1–28. https://doi.org/10.1016/j.quascirev.2013.08.014

NGRIP Members (North Greenland Ice Core Project Members), 2004. High-Resolution Record of Northern Hemisphere Climate Extending into the Last Interglacial Period. *Nature*, 431(7005): 147–151. https://doi.org/10.1038/nature02805

Rao, Z. G., Wu, D. D., Shi, F. X., et al., 2019. Reconciling the 'Westerlies' and 'Monsoon' Models: A New Hypothesis for the Holocene Moisture Evolution of the Xinjiang Region, NW China. *Earth-Science Reviews*, 191: 263–272. https://doi.org/10.1016/j.earscirev.2019.03.002

Shakun, J. D., Carlson, A. E., 2010. A Global Perspective on Last Glacial Maximum to Holocene Climate Change. *Quaternary Science Reviews*, 29(15/16): 1801–1816. https://doi.org/10.1016/j.quascirev.2010.03.016

Schnyder, J., Ruffell, A., Deconinck, J. F., et al., 2006. Conjunctive Use of Spectral Gamma-Ray Logs and Clay Mineralogy in Defining Late Jurassic – Early Cretaceous Palaeoclimate Change (Dorset, U. K.). *Palaeogeography*, *Palaeoclimatology*, *Palaeoecology*, 229(4): 303–320. https://doi.org/10.1016/j.palaeo.2005.06.027

Sun, J. M., Liu, W. G., Liu, Z. H., et al., 2017. Extreme Aridification since the Beginning of the Pliocene in the Tarim Basin, Western China. *Palaeogeography*, *Palaeoclimatology*, *Palaeoecology*, 485: 189–200. https://doi.org/10.1016/j.palaeo.2017.06.012

Sun, Y. B., Clemens, S. C., Morrill, C., et al., 2012. Influence of Atlantic Meridional Overturning Circulation on the East Asian Winter Monsoon. *Nature Geoscience*, 5(1): 46–49. https://doi. org/10.1038/ngeo1326

Wang, Y., Cheng, H. Y., Edwards, R., et al., 2002. A High-Resolution Absolute-Dated Late Pleistocene Monsoon Record from Hulu Cave, China. *Science*, 294(5550): 2345–2348. https://doi .org/10.1126/science.1064618

Wang, Y. J., Cheng, H., Edwards, R. L., et al., 2008. Millennial- and Orbital-Scale Changes in the East Asian Monsoon over the Past 224 000 years. *Nature*, 451(7182): 1090–1093. https://doi .org/10.1038/ nature06692

Wang, Y. J., Jia, J., Liu, H., et al., 2018. The Magnetic Susceptibility Recorded Millennial-Scale Variability in Central Asia during Last Glacial and Interglacial. *Geophysical Journal International*, 215(3): 1781–1788. https://doi.org/10.1093/gji/ggy378

Wu, L. X., Li, C., Yang, C. X., et al., 2008. Global Teleconnections in Response to a Shutdown of the Atlantic Meridional Overturning Circulation. *Journal of Climate*, 21: 3002–3019. http://doi.org/10.1175/2007JCLI1858.1

Wu, H. C., Zhang, S. H., Jiang, G. Q., et al., 2013. Astrochronology of the Early Turonian – Early Campanian Terrestrial Succession in the Songliao Basin, Northeastern China and Its Implication for Long-Period Behavior of the Solar System. *Palaeogeography*, *Palaeoclimatology*, *Palaeoecology*, 385: 55–70. https://doi.org/10.1016/j.palaeo.2012.09.004

XET-CAS (Xinjiang Expedition Team, Chinese Academy of Sciences), 1978. Vegetation and Its Utilization in Xinjiang. Science Press, Beijing (in Chinese)

Zhang, R., Li, L., Nai, W. H., et al., 2019. Astronomical Forcing of Terrestrial Climate Recorded in the Pleistocene of the Western Tarim Basin, NW China. *Palaeogeography*, *Palaeoclimatology*, *Palaeoecology*, 530: 78–89. https://doi.org/10.1016/j.palaeo.2019.05.039

Zhao, K. L., Li, X. Q., Dodson, J., et al., 2012. Climatic Variations over the Last 4000 Cal Yr BP in the Western Margin of the Tarim Basin, Xinjiang, Reconstructed from Pollen Data. *Palaeogeography*, *Palaeoclimatology*, *Palaeoecology*, 321/322: 16–23. https://doi.org/10.1016/j.palaeo.2012.01.012

Zheng, H. B., Wei, X. C., Tada, R., et al., 2015. Late Oligocene – Early Miocene Birth of the Taklimakan Desert. *Proceedings of the National Academy of Sciences of the United States of America*, 112(25): 7662–7667. https://doi.org/10.1073/pnas.1424487112